ORIGINAL PAPER

Theoretical study on aluminum carbide endohedral fullerene-$Al_4C@C_{80}$

Qi Liang Lu · Wen Jun Song · Jun Wei Meng · Jian Guo Wan

Abstract The possibility of a new endohedral fullerene with a trapped aluminum carbide cluster, $Al_4C @C_{80}$-I_h, was theoretical investigated. The geometries and electronic properties of it were investigated using density functional theory methods. The Al_4C unit formally transfers six electrons to the C_{80} cage which induces stabilization of $Al_4C@C_{80}$. A favorable binding energy, relatively large HOMO-LUMO gap, electron affinities and ionization potentials suggested the $Al_4C@C_{80}$ is rather stable. The analysis of vertical ionization potential and vertical electron affinity indicate $Al_4C@C_{80}$ is a good electron acceptor.

Keywords Aluminum carbide cluster · Density functional theory · Endohedral fullerenes

Introduction

Endohedral fullerenes have attracted tremendous attention and research interest from all over the world due to not only their novel structure but unique and outstanding properties [1–10]. The endohedral metal fullerenes (EMF), carbon cages embedding metal ions or clusters, are the most interesting subject. EMFs possess not only the physical and chemical properties of the carbon cage, but also unique properties of encapsulated

Q. L. Lu (✉) · W. J. Song · J. W. Meng
School of Physics and Material Science, Anhui University, Hefei 230039 Anhui, People's Republic of China
e-mail: qllufd@vip.sina.com

J. G. Wan
National Laboratory of Solid State Microstructures and Department of Physics, Nanjing University, Nanjing 210093 Jiangsu, People's Republic of China

atoms or clusters, such as magnetism, photoluminescence, quantum character, etc. [5, 11]. Moreover, EMFs have additional properties arising from metal–cage interactions [12, 13]. This will broaden their applications in biology, medicine, electronics and photovoltaics [14]. A unique feature of EMFs is the existence of substantial charge transfer from the encapsulated moiety to the cage. The transferred electrons can make some fullerenes of different sizes and symmetries that are relatively unstable become available for investigations [15–18]. For example, the C_{80} cage consists of 12 pentagons and 30 hexagons. There are seven isolated pentagon-rule satisfying structures (D_2, D_{5d}, C_{2v}(a), C_{2v}(b), D_3, D_{5h} and I_h) for the C_{80} cage [19, 20]. The I_h isomer is most unstable; however, it becomes stable upon charge transfer. Since the first discovery of trimetallic nitride template EMF, as exemplified by $Sc_3N@C_{80}$ in 1999 [11], many homologous metal cluster fullerenes were reported with different metal atoms or clusters inside the C_{80} cage, including metals nitride [11, 21–29], carbide [30–32], oxides [7, 33], hydrocarbide [34] and carbonitride [6]. We note that these metal atoms are all transition metal atoms. The properties of encapsulated transition metal clusters are determined by $3d$ and $4f$ orbitals. For aluminum carbide cluster, their properties are mainly governed by sp electrons. Hence, if $Al_4C@C_{80}$ is feasible, it will possess different properties from transition metal endofullerene. In this work, we will report a new non-transition metals carbide can be encapsulated in C_{80} and form a stable endohedral fullerene: $Al_4C@C_{80}$.

Computational methods

All the calculations are carried out within density functional theory (DFT) framework by using the $Dmol^3$ code [35]. In these calculations, an all electron treatment and double numerical polarized (DNP) basis sets are employed. The Perdew-Burke-Ernzerhof (PBE) functional [36] based on the generalized gradient approximation (GGA) is employed to

describe the exchange and correlation effects of electrons. We also compare the GGA results with those of the local density approximation (LDA) with Perdew-Wang (PWC) functional [37]. All structures are fully optimized with no symmetry restriction. Spin-unrestricted self-consistent field calculations are done with a convergence criterion of 10^{-5} a.u. on the total energy and electron density. We use convergence criteria of 0.004 Hartree/Å on the force parameters, 0.005 Å on the displacement parameter, and 2×10^{-5} Hartree on the total energy in the geometry optimization. To improve the convergence, thermal smearing is set at 0.0544 eV. Several different locations and orientations of the endohedral Al_4C clusters inside the fullerene cages are considered to survey the lowest energy structure of the EMFs. Vibrational frequency analysis are performed to check whether the structure is a true minimum without imaginary frequencies. In Dmol3, frequencies are evaluated by finite differences.

Results and discussion

Structures of seven Al_4C encapsulated C_{80} isomers are shown in Fig. 1 according to their relative energy. These species all have real frequencies and are minimum energy
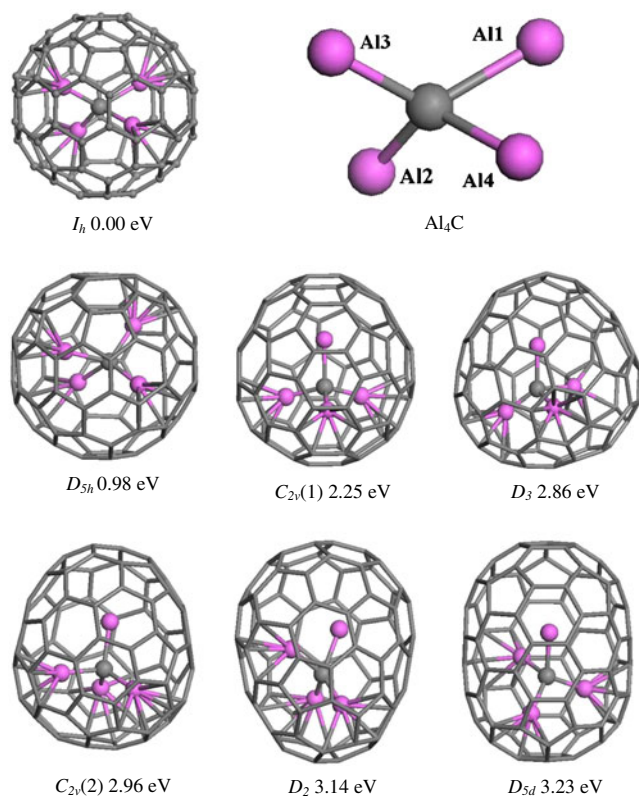

I_h 0.00 eV

Al_4C

D_{5h} 0.98 eV

$C_{2v}(1)$ 2.25 eV

D_3 2.86 eV

$C_{2v}(2)$ 2.96 eV

D_2 3.14 eV

D_{5d} 3.23 eV

Fig. 1 Optimized structures of seven Al_4C encapsulated C_{80} isomers according to their relative energy. The structure of the trapped Al_4C cluster is also given to the right of C_{80}-I_h. The symmetry group correspond to the free state C_{80} cage

structures along the potential energy surfaces. The structure of the trapped Al_4C cluster is also given. The most stable cage with D_2 symmetry is not the most stable structure after Al_4C inside it. An isomer with I_h symmetry is energetically the most favorable and thus has the ground-state structure. Only C_{80}-I_h cage, if not mentioned otherwise, will be discussed. The structures of several isomers of $Al_4C@C_{80}$-I_h, in which the Al_4C cluster is placed at different locations and with different orientations inside the C_{80}-I_h cage, have been optimized. It results in multiple conformers with close relative energies. The given structure is the lowest energy conformer with C_1 symmetry. In this structure, two Al atoms face the centers of the hexagon, while the other two Al atoms connect the midpoints of the pentagon. The structure with only one Al atom facing the centers of the pentagon is only 0.005 eV less stable than the lowest energy conformer. For the most stable structure, the nearest distance between Al atoms and the cage (R) are present in Table 1. The bond lengths of Al-C (r) within the cluster are also summarized in this table. From these data of R, we can see that Al_4C cluster is somewhat displaced toward one side of the cage.

The free Al_4C molecule is tetrahedral with an optimized Al-C bond length of 2.02 Å (ref. [38] and [39] confirmed that the structure of this molecule is tetrahedral pattern and given the Al-C bond length of 2.01 Å at B3LYP/6-311+G^* level) and an Al-C-Al bond angle of 110° at present level of theory. When an Al_4C unit is encapsulated by C_{80} cage, there is a significant distortion in the structure of it (see Fig. 1). The inner C atom nearly locates at the center of the C_{80} cage. As shown in Table 1, the computed Al-C bond length (r) of trapped Al_4C cluster is significantly different from that of the free state. The mean r is found to be 2.06 Å, slightly shorter than that of free Al_4C cluster. We can see from this table that the closer the distance between Al atom and the cage, the smaller the Al-C bond length, but values of the latter are remarkably smaller than those of their counterpart. Thus the interaction between Al atoms and the C atom of the cluster is stronger than that between the Al atoms and the C_{80} cage.

Note that C_{80}-I_h has the four-fold degenerate unfilled at the highest occupied molecular orbital (HOMO) (see Fig. 2).

Table 1 R is the distance between Al atom and C atom of the C_{80} cage (in angstrom). One Al atom can interact with several C atoms. The R refer to the nearest one. r is the bond length of Al-C within Al_4C cluster (in angstrom)

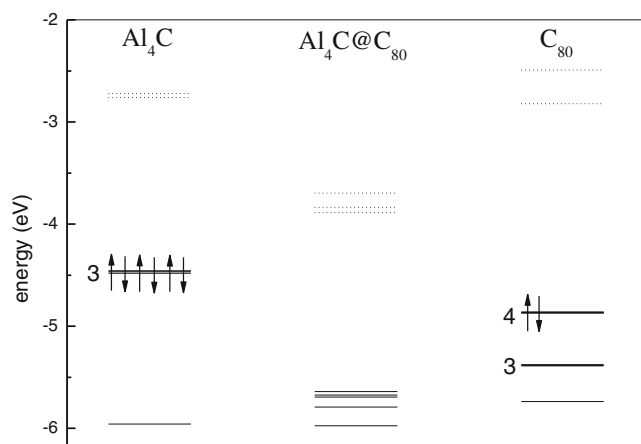|	R (Å)	r (Å)
Al1	2.35	2.14
Al2	2.20	1.99
Al3	2.16	1.98
Al4	2.28	2.13

Fig. 2 Molecular orbital levels of Al_4C, $Al_4C@C_{80}$ and C_{80}. Only the most important levels that participate in the interaction are given. Occupied levels are solid, unoccupied levels are dot. A number 3 and 4 indicates the degeneracy type for electron levels
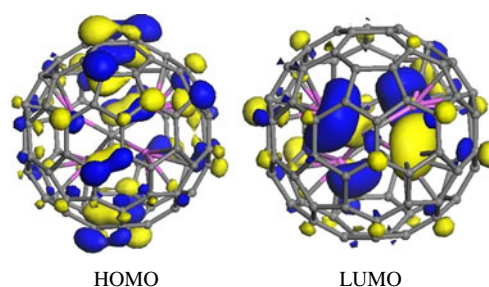

Fig. 3 The charge density of the highest occupied molecular orbital (HOMO) and the lowest unoccupied molecular orbital (LUMO) at iso-value of 0.03 electron/$Å^3$

Two electrons occupy the four HOMOs. Hence, only one HOMO level is filled and three of them remain empty. When Al_4C interacts with the HOMO of C_{80}, the orbital is now filled with the six electrons from the HOMO of Al_4C leading to a closed shell status for the $Al_4C@C_{80}$. The filled level induced by Al_4C lies at about -5.67 eV. The downward shifts the level result in a sizable HOMO-LUMO gap (1.75 eV) of $Al_4C@C_{80}$. A large gap can imply its substantial kinetic stability because it is energetically unfavorable to add electrons to a high-lying LUMO or to extract electrons from a low-lying HOMO. The orbital interaction diagram of Fig. 2 clearly shows a formal transfer of six electrons from the HOMO of Al_4C cluster to the C_{80} cage. So the valence state of $[Al_4C]^{6+}$ @$[C_{80}]^{6-}$ can be assigned to the $Al_4C@C_{80}$, as observed for other stable C_{80}-I_h based endohedral metal fullerenes such as $[Sc_3N]^{6+}$ @$[C_{80}]^{6-}$. For the absorption of light, the initial position of spectrum depend on energy difference between HOMO and LUMO [21, 22, 40, 41]. The photovoltaic process begins with light absorption and ends with charge transport to the electrodes. It has to be around 2 eV as this corresponds to the maximum in the solar radiation energy spectrum [42]. For the $Al_4C@C_{80}$, the HOMO-LUMO gap is smaller than 2 eV, and therefore, it could be useful for the construction of solar cells.

The HOMO of $Al_4C@C_{80}$ is predominately delocalized on the carbon cage as seen in Fig. 3. It is analogous to those of endohedral transition metal cluster fullerenes (i.e., $Sc_3N@C_{80}$ [43]). While for the LUMO, it is mainly localized around Al atoms. The cage contribution to the LUMO of $Al_4C@C_{80}$ is very small. The redox properties of $Al_4C@C_{80}$ will be dominated by these frontier orbitals. The LUMO orbitals are mainly localized around Al atoms. As a result, the added electrons in the reduction states $[Al_4C@C_{80}]^q$ (q=−1, -2) are mainly distributed on Al atoms whereas the valence state of the cage is kept at $[C_{80}]^{6-}$. The charge state of Al_4C and the Al-C bond

length will change. On the contrary, for the oxidation states of $[Al_4C@C_{80}]^q$ (q=+1, +2), the lost electrons are mostly derived from the C_{80} cage due to the HOMO orbital mainly located on it. Hence, the charge state of Al_4C cluster is unchanged. The valence state of the cage will be $[Al_4C@C_{80}]^{(6-q)-}$.

Mulliken population given in Table 2 shows that Al and C atoms of Al_4C are all involved in the charge transfer. However, this process is predominately dominated by Al atoms, C atom plays minor role. Furthermore, there are a large number of populations on d orbitals of Al atoms. Populations of free Al_4C molecules show that C atom is strongly negatively charged with $-0.85e$ and a positive charge of $0.21e$ locating on Al atoms. Isolated state Al_4C has very similar values to those of its free state. It is noted that the difference of charge on C atom between the four states is small. Comparison with isolated Al_4C, a lowering of $0.62e$ in $3s$ orbitals and increasing of $0.32e$ in $3d$ orbitals of each Al atom can be found when the unit is encapsulated in the cage. As a result, the total charge of each Al atom in the endohedral fullerene reaches $0.67e$, but the magnitude is much smaller than that of isolated Al_4C^{6+} ($1.71e$). The total charge transfer between Al_4C and the C_{80} cage is $1.75e$. It implies that the charge transfer is not so important for stabilization of the endohedral fullerene $Al_4C@C_{80}$. The C_{80} cage is negatively charged due to quite an amount of charge transfer between the two units. The changes in charge can be identified by visualization of the spatially deformed charge distribution in the endohedral fullerene, which is defined as the total charge density minus the density of the isolated atoms. The electronic character of $Al_4C@C_{80}$ at an iso-value of 0.20 $e/Å^3$ is illustrated in Fig. 4. The figure clearly shows that a large amount of difference charge is on the C_{80} cage and mainly distributed between two C atoms. This tells us that there is covalency in C-C interactions. The fact that a small amount of the charge distributed on the Al_4C moiety is consistent with the Mulliken populations.

The binding energy of the Al_4C cluster to the C_{80} cage (E_b) is calculated according to the following expression:

$$-E_b = E(Al_4C@C_{80}) - E(Al_4C) - E(C_{80}),$$

Table 2 Mulliken population for the Al₄C cluster with different states. Isolated Al₄C and Al₄C⁶⁺ have the same structure as that of trapped Al₄C. The structure of free Al₄C molecule is tetrahedral

	Al				C		
	net charge	3s	3p	3d	net charge	2s	2p
trapped Al₄C	0.67	1.17	0.72	0.44	−0.93	1.64	3.29
isolated Al₄C	0.18	1.79	0.91	0.12	−0.73	1.47	3.26
isolated Al₄C⁶⁺	1.71	0.89	0.29	0.11	−0.84	1.59	3.25
free Al₄C	0.21	1.86	0.82	0.11	−0.85	1.47	3.38

which represents a gain in energy as Al_4C is trapped in C_{80}. This is a signature quality of the stability of endohedral fullerene. Results also imply that the encapsulation process of Al_4C into the cage is an exothermic process that yields a binding energy of 0.30 eV at GGA level, but LDA gives the result of 0.86 eV. This magnitude indicates the weak interaction between the cluster and the cage. It is widely known that GGA usually underestimates while LDA overestimates the binding strength [44–46]. The real binding energy may intermediate the results of GGA and LDA.

Calculations were also carried out to compute their vertical ionization potential (VIP), vertical electron affinity (VEA) as well as adiabatic ionization potential (AIP) and adiabatic electron affinity (AEA). The computed IP are 6.92 eV (VIP) and 6.91 eV (AIP), while values of EA are 2.55 eV (VEA) and 2.77 eV (AEA). The VIP and VEA of $Al_4C@C_{80}$ are analogous to those of $Sc_3N@C_{80}$ [43, 47]. (Results of ref. [43] are 6.88 eV and 2.99 eV, while VEA of ref. [47] is 2.81 eV.) It suggests that the $Al_4C@C_{80}$ has good electron accepting capacity.

Studies shown that hollow fullerene are good electron acceptor organic materials [48]. The combination of fullerene and some organometallic molecule can provide nanostructures for opto-electronic devices of the p (an electron acceptor)-n (an electron donor) junction type [49–51]. Studies found that some EMF have better electron accepting power than hollow fullerene [52, 53]. The HOMO orbital mainly locate on C_{80} cage, these active centers can adsorb other organometallic molecules, and form a electron donor-acceptor system. It is interesting to discuss the donor-
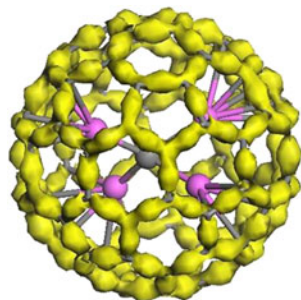
acceptor properties of $Al_4C@C_{80}$. A model was proposed to evaluate donating and accepting capacity of a system [42, 54–56]. The donate and accept electron power can be defined as:

$$\omega^- = \frac{(3VIP + VEA)^2}{16(VIP - VEA)} \text{ and } \omega^+ = \frac{(VIP + 3VEA)^2}{16(VIP - VEA)}.$$

Chose F and Na atoms for reference as a good electron acceptor and donor. An electron acceptance index can be defined as $R_a = \omega^+/\omega_F^+$. $R_a > 1$ means $Al_4C@C_{80}$ has better accepting power than F atom. An electron donation index is defined as $R_d = \omega^-/\omega_{Na}^-$ [54, 55]. If $R_d > 1$, $Al_4C@C_{80}$ is a worse electron donor than Na atom. The VIP and VEA of F atom obtained at the same level of theory are 17.84 eV and 2.84 eV. These values of Na atoms are 5.02 eV and 1.03 eV, respectively. It can be obtained $R_a = 1.05$ and $R_d = 1.91$. These data show that $Al_4C@C_{80}$ is a good electron acceptor and a bad electron donor.

Conclusions

In summary, a endohedral fullerene trapping non-transition metals carbide, namely, $Al_4C@C_{80}$, were reported by means of DFT calculations. The C_{80} fullerene with I_h symmetry is energetically the most favorable after Al_4C is inside it. In the lowest energy structure, two Al atoms face the centers of the hexagon, while the other two Al atoms connect the midpoints of the pentagon. Molecular orbital analysis revealed that formal charge transfer of $6e$ from Al_4C unit to the C_{80} cage induces stabilization for $Al_4C@C_{80}$. $Al_4C@C_{80}$ holds a large HOMO-LUMO gap of 1.75 eV and a favorable binding energy, implying its promise for experimental realization. The analysis of VIP and VEA indicate $Al_4C@C_{80}$ is a good electron acceptor and a bad electron donor. It is well known that the properties of nanoclusters are very sensitive to their structure and composition. Studies have shown that encapsulated atoms or clusters can remarkably affect the properties of EMF [27, 57–60]. It is expected that the properties of $Al_4C@C_{80}$ will be significantly different from those of endohedral fullerene trapping transition metal atoms, and should be further investigated.

Fig. 4 Deformation electron density of $Al_4C@C_{80}$ at an iso-value of 0.02 electron/Å³

References

1. Chaur MN, Athans AJ, Echegoyen L (2008) Tetrahedron 64:11387–11393
2. Heath JR, Obrien SC, Zhang Q, Liu Y, Curl RF, Kroto HW, Tittel FK, Smalley RE (1985) J Am Chem Soc 107:7779–7780
3. Alvarez MM, Gillan EG, Holczer K, Kaner RB, Min KS, Whetten RL (1991) J Phys Chem 95:10561–10563
4. Stevenson S, Fowler PW, Heine T, Duchamp JC, Rice G, Glass T, Harich K, Hajdu E, Bible R, Dorn HC (2000) Nature 408:427–428
5. Wang CR, Kai T, Tomiyama T, Yoshida T, Kobayashi Y, Nishibori E, Takata M, Sakata M, Shinohara H (2001) Angew Chem Int Ed 40:397–399
6. Wang TS, Feng L, Wu JY, Xu W, Xiang JF, Tan K, Ma YH, Zheng JP, Jiang L, Lu X, Shu CY, Wang CR (2010) J Am Chem Soc 132:16362–16364
7. Stevenson S, Mackey MA, Stuart MA, Phillips JP, Easterling ML, Chancellor CJ, Olmstead MM, Balch AL (2008) J Am Chem Soc 130:11844–11845
8. Saunders M, Jimenezvazquez HA, Cross RJ, Poreda RJ (1993) Science 259:1428–1430
9. Komatsu K, Murata M, Murata Y (2005) Science 307:238–240
10. Ramachandran CN, Sathyamurthy N (2005) Chem Phys Lett 410:348–351
11. Stevenson S, Rice G, Glass T, Harich K, Cromer F, Jordan MR, Craft J, Hadju E, Bible R, Olmstead MM, Maitra K, Fisher AJ, Balch AL, Dorn HC (1999) Nature 401:55–57
12. Yamada M, Akasaka T, Nagase S (2010) Acc Chem Res 43:92–102
13. Sun BY, Li MX, Luo HX, Shi ZJ, Gu ZN (2002) Electrochim Acta 47:3545–3549
14. Lu X, Feng L, Akasaka T, Nagase S (2012) Chem Soc Rev doi:10.1039/c2cs35214a
15. Beavers CM, Zuo T, Duuchamp JC, Harich K, Dorn HC, Olmsread MM, Balch AL (2006) J Am Chem Soc 128:11352–11353
16. Yang S, Popov AA, Dunsch L (2007) Angew Chem Int Ed 46:1256–1259
17. Lu X, Akasaka T, Nagase S (2011) Chem Commun 47:5942
18. Yang S, Liu F, Chen C, Jiao M, Wei T (2011) Chem Commun 47:11822
19. Manolopoulos DE, Folwer PW (1992) J Chem Phys 96:7603–7614
20. Kobayashi K, Nagase S, Akasaka T (1995) Chem Phys Lett 245:230–236
21. Chaur MN, Melin F, Ortiz AL, Echegoyen L (2009) Angew Chem Int Ed 48:7514–7538
22. Dunsch L, Yang SF (2007) Small 3:1298–1320
23. Stevenson S, Phillips JP, Reid J E, Olmstead MM, Rath SP, Balch AL (2004) Chem Commun 2814–2815
24. Yang SF, Dunsch L (2005) Chem Eur J 12:413–419
25. Dunsch L, Krause M, Noack J, Georgi P (2004) J Phys Chem Solids 65:309–315
26. Chen N, Zhang EY, Wang CR (2006) J Phys Chem B 110:13322–13325
27. Chen N, Fan LZ, Tan K, Wu YQ, Shu CY, Xin L, Wang CR (2007) J Phys Chem C 111:11823–11828
28. Stevenson S, Chancellor CJ, Lee HM, Olmstead MM, Balch AL (2008) Inorg Chem 47:1420–1427
29. Yang SF, Chen CB, Popov AA, Zhang WF, Liu FP, Dunsch L (2009) Chem Commun 6391–6393
30. Iiduka Y, Wakahara T, Nakahodo T, Tsuchiya T, Sakuraba A, Maeda Y, Akasaka T, Yoza K, Horn E, Kato T, Liu MTH, Mizorogi N, Kobayashi K, Nagase S (2005) J Am Chem Soc 127:12500–12501
31. Wang TS, Chen N, Xiang JF, Li B, Wu JY, Xu W, Jiang L, Tan K, Shu CY, Lu X, Wang CR (2009) J Am Chem Soc 131:16646–16647
32. Kurihara H, Lu X, Iiduka Y, Mizorogi N, Slanina Z, Tsuchiya T, Akasaka T, Nagase S (2011) J Am Chem Soc 133:2382–2385
33. Mercado BQ, Olmstead MM, Beavers CM, Easterling ML, Stevenson S, Mackey MA, Coumbe CE, Phillips JD, Phillips JP, Poblet JM, Balch AL (2010) Chem Commun 46:279–281
34. Krause M, Ziegs F, Popov AA, Dunsch L (2007) Chemphyschem 8:537–540
35. Delley B (1990) J Chem Phys 92:508–517
36. Perdew JP, Burke K, Ernzerhof M (1996) Phys Rev Lett 77:3865–3868
37. Perdew JP, Wang Y (1992) Phys Rev B 45:13244–13249
38. Li X, Wang LS, Boldyrev AI, Simons J (1999) J Am Chem Soc 121:6033–6038
39. Zubarev DY, Boldyre AI (2005) J Chem Phys 122:144322
40. Shinohara H (2000) Rep Prog Phys 63:843–892
41. Yang SF, Dunsch L (2008) "Endohedral fullerenes", nanomaterials. In: Lukehart CM, Scott RA, (eds) Inorganic and bioinorganic perspectives. Wiley, Chichester
42. Ramos E, Monroy BM, Alonso JC, Sansores LE, Salcedo R, Martínez A (2012) J Phys Chem C 116:3988–3994
43. Campanera JM, Bo C, Olmstead MM, Balch AL, Poblet JM (2002) J Phys Chem A 106:12356–12364
44. Kim YH, Zhao YF, Williamson A, Heben MJ, Zhang SB (2006) Phys Rev Lett 96:016102
45. Okamoto Y, Miyamoto Y (2001) J Phys Chem B 105:3470–3474
46. Gao Y, Zeng XC (2007) J Phys Condens Matter 19:386220
47. Ioffe IN, Boltalina OV, Sidorov LN, Dorn HC, Stevenson S, Rice G (2000) In: Kadish KM, Ruoff RS (eds) Fullerenes: Recent advances in the chemistry and physics of fullerenes and related materials. Electrochemical Society, Pennington, p 166
48. Langa F, Nierengarten JF (2007) Fullerenes: Principles and applications. Royal Society of Chemistry, Oxford
49. Guldi DM, Illescas BM, Atienza CM, Wielopolski M, Martín N (2009) Chem Soc Rev 38:1587–1597
50. Bottari G, de la Torre G, Guldi DM, Torres T (2010) Chem Rev 110:6768–6816
51. Quintiliani M, Kahnt A, Wöfle T, Hieringer W, Vázquez P, Görling A, Guldi DM, Torres T (2008) Chem Eur J 14:3765–3775
52. Ross RB, Cardona CM, Guldi DM, Sankaranarayanan SG, Reese MO, Kopidakis N, Peet J, Walker B, Bazan GC, Keuren EV, Holloway BC, Drees M (2009) Nat Mater 8:208–212
53. Ross RB, Cardona CM, Swain FB, Guldi DM, Sankaranarayanan SG, Keuren EV, Holloway BC, Drees M (2009) Adv Funct Mater 19:2332–2337
54. Martínez A, Rodríguez-Gironés MA, Barbosa A, Costas M (2008) J Phys Chem A 112:9037–9042
55. Martínez A, Galano A (2010) J Phys Chem C 114:8184–8191
56. Gázquez JL, Cedillo A, Vela A (2007) J Phys Chem A 111:1966–1970
57. Yang SF, Popov A, Kalbac M, Duusch L (2008) Chem Eur J 14:2084–2092
58. Yang SF, Popov AA, Chen CH, Dunsch L (2009) J Phys Chem C 113:7616–7623
59. Tarabek J, Yang SF, Dunsch L (2009) Chemphyschem 10:1037–1043
60. Zhang L, Popov A, Yang SF, Klod S, Rapta P, Dunsch L (2010) Phys Chem Chem Phys 12:7840–7847